CrystEngComm

Solvothermal Synthesis of Porous Organic Cage CC3 in the Presence of Dimethylformamide as Solvent

Journal:	*CrystEngComm*
Manuscript ID	CE-COM-04-2019-000662.R2
Article Type:	Communication
Date Submitted by the Author:	19-Jul-2019
Complete List of Authors:	Lucero, Jolie; Colorado School of Mines Crawford, James; COLORADOSCHOOLOFMINES, Chemical and Biological Engineering Osuna, Carla; Colorado School of Mines Carreon, Moises; COLORADOSCHOOLOFMINES, Chemical and Biological Engineering

Solvothermal Synthesis of Porous Organic Cage CC3 in the Presence of Dimethylformamide as Solvent

Jolie Lucero, James M. Crawford, Carla Osuna, Moises A. Carreon *

Department of Chemical and Biological Engineering, Colorado School of Mines, Golden, Colorado 80401, United States;

*Corresponding author: mcarreon@mines.edu

ABSTRACT

A prototypical porous organic cage denoted as CC3 was synthesized in the presence of dimethyformamide as solvent. Stirring effects and solvothermal treatment conditions lead to distinctive morphological, structural, and textural properties of the resultant CC3 crystals. The presence of DMF led to a mixture of alpha and dissymmetric cage structures. The crystallinity of the resulting crystals was highly dependent on the solvothermal temperature.

Porous organic cages (POCs) are an emerging class of functional porous crystalline materials which exhibit highly desirable properties such as high surface areas,[1, 2] uniform micropores,[3] thermal and chemical stability,[1, 4] and solution processability,[5] making them suitable for diverse functional applications in different fields including chemical separations,[6] gas adsorption,[7] heterogeneous catalysis,[8, 9] and sensing.[3] The unique solid state packing of the discreet POC molecules give rise to highly desirable properties which can be easily tuned.[10] The prototypical POC, CC3, is typically synthesized from the trialdehyde - 1,3,5-triformylbenzene, and a chiral ((±)-trans, R,R-(-), or S,S-(+)) 1,2- diaminocyclohexane in a 4:6 molar ratio in the presence of dichloromethane or chloroform as solvents. The racemic mixture of the trans diamine is preferred, due to a reduction in cost, and increased resistance to acid gas of the final mixed racemate cage product.[11] Recently, it has been shown, that use of the racemate diamine will yield 4 types of CC3 cage products, a co-crystal precipitate, CC3-R/CC3-S, comprised of homochiral CC3-R and CC3-S cages, and heterochiral cages CC3-SR, and CC3-RS.[5, 12] This cage has a pore cavity of 4.4 Å, a limiting pore windows of 3.6 Å, making it highly attractive for noble gas separations, in particular Xe/Kr.[13, 14] If the heterochiral and homochiral cage products were separated, their crystalline phases would reveal different space group symmetries.[5,12] Homochiral CC3-R has been well known to thermodynamically favor the CC3α phase,[2] packing in a window-to-window arrangement, and produce 3D diamondoid pores within FCC crystals. The co-crystal precipitates quickly out of solution following its formation, [15] due to the energetically favorable chiral recognition between the two opposing homochiral cages.[15, 16] The heterochiral cages however, remain soluble in the synthesis solution, but can be precipitated using hexane to crystallize in a trigonal space group ($R\bar{3}$) symmetry.[5] The apparent Brunauer Emmet Teller (BET) surface area of CC3α ranges from ~409-819 m^2/g, depending on the speed of crystallization,[15] while the SA_{BET} of the heterochiral cage product is ~800 m^2/g [5] .

Morphological control over crystal size, shape, intergrowth, and phase has been shown to be important in applications such as membrane synthesis,[17, 18] and catalysis,[19, 20] among others. Morphological control of other types of porous crystalline materials, such as zeolites and metal organic frameworks, has been accomplished typically through the use of additives, [21, 22] solvent environment, [23] and solvothermal treatment.[24] Recent computational studies[25-27] have aimed at

discovering new porous organic cages through the use of new algorithms and the investigation of solvent effects. There are few emerging experimental studies on defect and morphological control in POCs, [15, 28-30] but control using the latter mentioned methods are lacking for this class of materials.

The central objective of this study, is to tune the morphological, structural, and textural properties of CC3-R/CC3-S by an in situ solvothermal synthesis approach, employing a non-traditional solvent for the synthesis of POC CC3. Specifically, N, N-Dimethylformamide (DMF) was employed as solvent for the growth of CC3 crystals. The rational of using DMF as solvent is because of its polar aprotic nature, and high dielectric constant, which can readily dissolve trialdehydes. We report the effect of stirring, and solvothermal treatment on the morphology and formation of CC3-racemate crystals. Through solvothermal treatment, we demonstrate the formation of CC3-racemate crystals *in situ*, and an increase of heterochiral cages with solvothermal treatment time. Our experimental findings corroborate with the *in silico* CC3-racemate models reported by Liu *et al.,* [12] and experimentally show how these molecules pack and nucleate to form large racemic crystals from the desolvation of only one solvent. To the best of our knowledge this is the first evidence of preparation of CC3-R/CC3-S, and CC3-RS/CC3-SR, using this synthetic approach, and solvent.

The CC3-R/CC3-S in this study was synthesized using the procedure described in the ESI.† To determine the effect of mixing on cage formation in DMF, two experiments were performed at room temperature for 4 days. The first experiment entailed the slow addition of the diamine solution to the aldehyde solution to prevent mixing. The second experiment involved mixing the two solutions on a stir plate at 300 rpm. After 4 days, each sample was separated by centrifugation, washed with clean DMF 3X, and dried overnight in a vacuum oven at 110°C. These experiments allow us to elucidate the effect of stirring in the formation of CC3 crystals. In a second set of experiments, we evaluated the effect of solvothermal treatment time on the formation of CC3. Specifically, the mixed solution was added to a Teflon lined autoclave and treated in an oven at 100°C for various times.† Detailed characterization techniques are described in the ESI.†

PXRD was used to characterize the crystalline phases of each sample synthesized in the presence of DMF. The powder diffraction data along with calculated powder patterns of CC3α, [1] is shown in **Figure 1.** Both samples synthesized at room temperature with and without stirring, display broad peaks which match with the position of the calculated peaks corresponding to CC3α structure. The room temperature stirred sample shows a slight increase in relative crystallinity, especially in the most prominent CC3α peak corresponding to the plane (2 2 2) at 2θ~12.4°. The broad peaks in these samples suggest amorphous character, [15] likely resulting from defects in crystal packing, and local structural disorder.[31]

Figure 2 shows representative SEM images of non-stirred and stirred CC3 crystals. The effect of stirring vs non-stirring of the synthesis solution at room temperature is evident. The crystallites shown in **Figure 2.a** are homogenous ~1.1 ± 0.5 μm in size (quantified by SEM), displaying spherical morphology. **Figure 2.b** is the stirred sample with a crystal size of ~1.2 ± 0.5 μm, and faceted octahedral crystals - the typical morphology of CC3. In the presence of DMF, stirring had a profound effect on the kinetics of cage formation, and morphology of the resultant crystals. Stirring affects the kinetics by which the solutes will dissolve in the solvent. Specifically, the kinetics of saturation will be different for the non-stirred vs stirred case, leading to distinctive crystal growth which is reflected in the final morphology of the crystals (sphere-like vs octahedral-like). Stirring allows a better interaction between the solutes and solvent leading to rapid

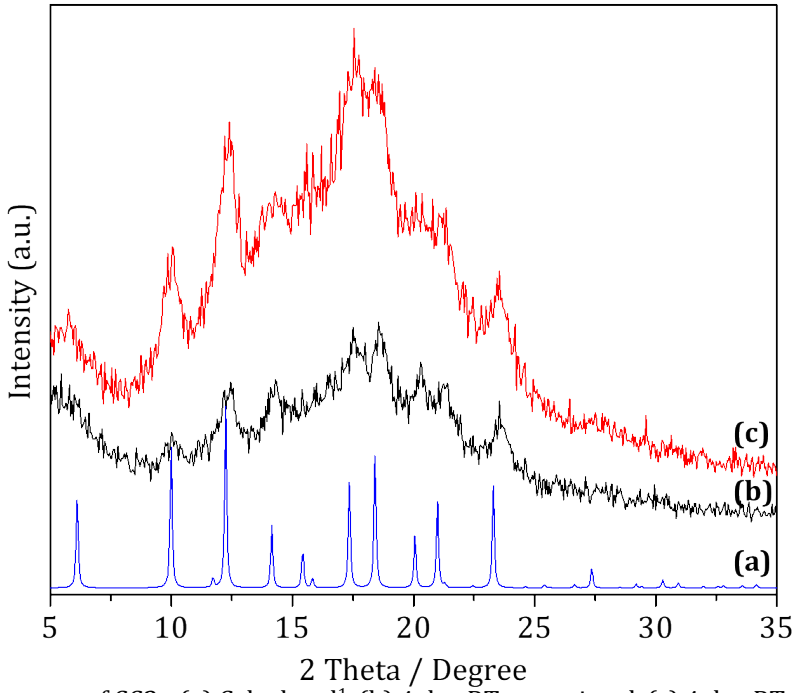

Figure 1. PXRD patterns of CC3α (a) Calculated[1], (b) 4 day RT non-stirred, (c) 4 day RT stirred.

precipitation of CC3-R/CC3-S. In the absence of stirring, the concentration of solutes is high, and gradually decreases, while in the stirring case, this concentration rapidly decreases and become steady (**Figure S1**). The kinetics of this concentration gradient should affect the overall crystallization process affecting the resultant crystal size, shape, and distribution. In principle, the most thermodynamically stable, and simplest form that a colloidal particle can adopt in solution during nucleation and growth is the spherical shape. In the non-stirred case, this shape is likely preferred due to: (a) the higher concentration of solutes leading to a faster supersaturation (solute concentration/solubility ratio), and (b) lower local thermal energy associated to the stagnant solution (non-stirred case) leading to the lowest energy spherical shape configuration. The formation of CC3 spherical shapes has been documented previously.

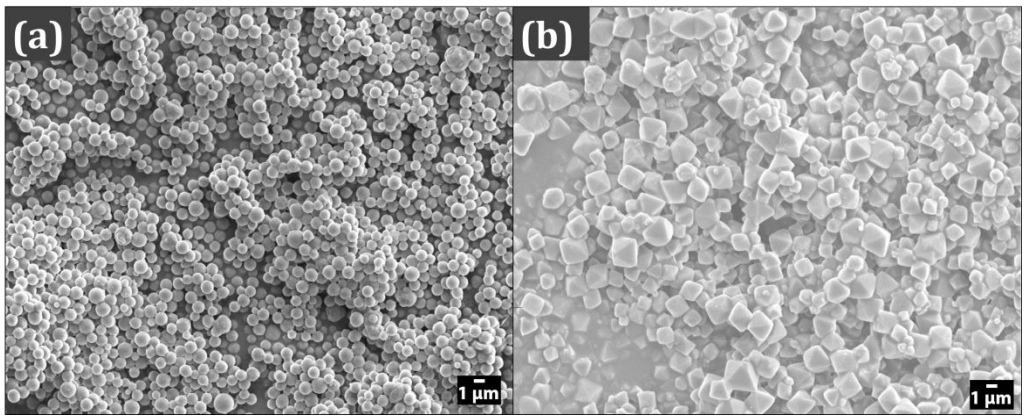

Figure 2. SEM images of CC3 crystals (a) 4 day RT non-stirred, (b) 4 days stirred.

Hasell *et al.*[15] described morphological changes by mixing dissolved solutions of pre-synthesized, pure chiral CC3-R, and CC3-S in DCM at different rates. In this report, the authors obtain CC3-R/CC3-S precipitates which are spherical with rapid mixing, and octahedral crystals with slow mixing of chiral cages.

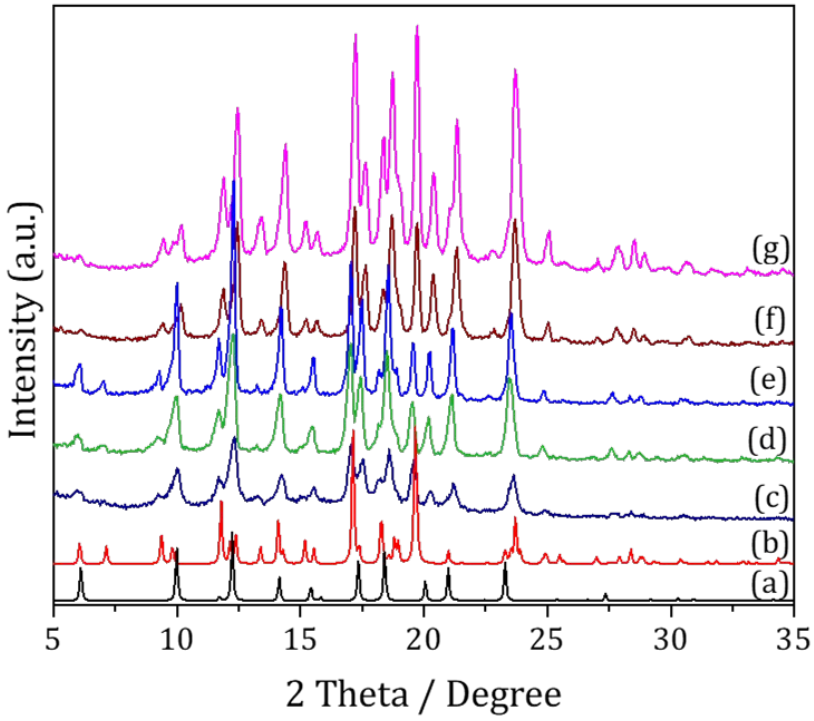

Figure 3. PXRD patterns of (a) calculated CC3 α,[1] (b) calculated CC3-SR/CC3-RS,[5] (c) 3 day RT stir + 12h@100°C solvothermal, (d) 3 day RT stir + 12h@100°C +12h@50°C solvothermal, (e) 3 day RT stir +16h@100°C solvothermal, (f) 3 day RT stir + 24h@100°C solvothermal, (g) 3 day RT stir + 3d@100°C solvothermal.

Figure 3 shows PXRD patterns for CC3 samples synthesized solvothermally for different times at 100°C.† Incremental increases of time for solvothermal treatment lead to sharper narrowing of peaks in the patterns (as compared to the samples synthesized only at room temperature) suggesting enhanced crystallinity. Interestingly, this data along with SEM imaging, and refinement calculations, (**Figure S2**), confirms that a mixture of CC3α, and heterochiral CC3-RS/CC3-SR crystals are present in these samples, which is apparent by the appearances of peaks at 2θ~7°, 2θ~13.5°, 2θ~18.1°, 2θ~18.7°, 2θ~19.4°, 2θ~23°, and 2θ~24.9°. From our previous study, [28] the observed slight peak shifts for some of these samples to lower 2θ angles, originate from unit cell changes in the CC3 crystal. Furthermore, the co-existence of the two types of cages is well documented.[5, 12] **Figure S3** shows the TGA profiles for the synthesized CC3 samples. All samples synthesized exhibit thermal stability up to ~325°C. This temperature is comparable to the thermal stability of CC3 crystals synthesized in the presence of DCM.[1]

FTIR spectra in **Figure S4** confirm CC3 conformation in all samples.[1] With extended solvothermal treatment, the product yield of CC3-racemic steadily increased up to 60%,† due to the

addition of heating to promote reversibility of the Shiff type reaction in the absence of an acid catalyst.[31]

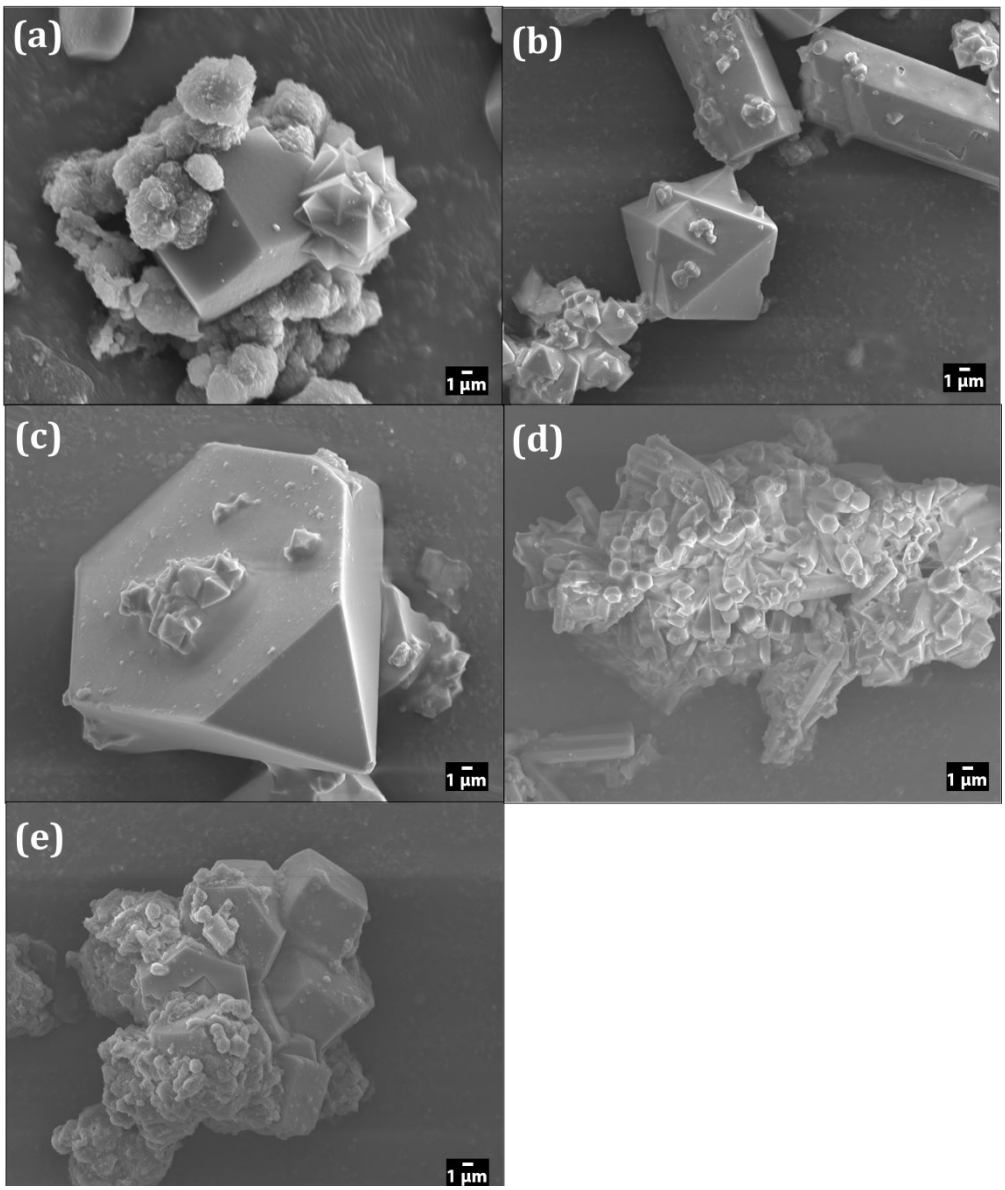

Figure 4. SEM images of solvothermally treated samples. (a**)** 3 day RT stir + 12h@100°C solvothermal, (b) 3 day RT stir + 12h@100°C +12h@50°C solvothermal, (c) 3 day RT stir + 16h@100°C solvothermal, (d) 3 day RT stir + 24h@100°C solvothermal, (e) 3 day RT stir + 3d@100°C solvothermal. All scale bars are 1 µm.

The heterochiral CC3-RS/CC3-SR crystals exhibit a trigonal crystal system and space group $R\bar{3}$, [5] while CC3α, when synthesized in DCM, (CC3-R, CC3-S, and CC3-R/CC3-S) crystallizes in an octahedral morphology with a cubic space group $F4_132$.[1,2] The morphology of the heterochiral crystals has not been well documented due to the very small crystals obtained through the hexane precipitation method.[5] **Figure 4** depicts the morphology of the CC3-racemic crystals as a function of solvothermal treatment time. Upon close inspection of **Figure 4.a**, a mixture of large and submicron sized octahedral crystals, along with a large hexagonal-like crystal, are efficiently intergrown.

Samples (b), and (c) illustrate the growth progression of the CC3-SR/CC3-RS crystals with prolonged solvothermal treatment. Extended solvothermal treatment, ((d) and (e)), resulted in steady growth due to Ostwald Ripening of crystals up to a maximum of ~80 μm, and a larger population of hexagonal crystals. This observation was confirmed by analyzing the PXRD patterns, (f), and (g) in **Figure 3**. The overall patterns had a large contribution from the CC3-RS/CC3-SR crystals, based off the steady increase in intensity of the most prominent peaks of the heterochiral cage crystals at 2θ~17.1°, and 2θ~19.7°. Treatment for 24 hours resulted in improved crystal intergrowth of the racemic crystal.

In our DMF solvothermal system, a higher concentration of heterochiral cages are being produced over the homochiral cages to form the co-crystal α-phase precipitate. We hypothesize that this may be due to the prolonged heating step during the solvothermal synthesis, since this increases the reversibility of the Shiff type reaction as mentioned earlier.[31] In principle, the cages have a longer time to repeatedly form, and break down, allowing more time for the cages to exchange linkers in a dissymmetric fashion to allow the formation of the heterochiral cages. Because DMF is a more effective solvent in terms of dielectric constant, and ability to solubilize TFB, the cage molecules during hydrothermal synthesis take longer to form because of higher linker-DMF interactions rather than linker-linker interactions. Homochiral cages are not formed as easily with the addition of heat and DMF, therefore co-crystal precipitates are formed in lower yields. Additional SEM images are shown in **Figures S5-S11**. The synthesized CC3 samples in the presence of DMF displayed the typical high surface areas reported for this POC.[2, 12] Specifically, Brunauer-Emmet-Teller (BET) surface areas of 462 m^2/g, 511 m^2/g, 525 m^2/g, 410 m^2/g, 452 m^2/g, 438 m^2/g, 401 m^2/g were collected from N_2 adsorption/desorption isotherms (**Figure S12**) for samples (a)-(g) respectively. Although sample (a) does not show well defined crystallinity in the PXRD patterns, it shows a relatively high surface area. In principle, the relative low crystallinity of this sample leads to inefficient packing, reducing the density of the material, and creating gaps among the cages leading to additional adsorption sites for nitrogen, and therefore to higher observed surface areas.[22] Sample (c) has a surface area very close to that of pure CC3β-R,[2] because CC3-SR/CC3-RS and CC3β both pack into 1D pore channels.[2, 5] Pure CC3-SR/CC3-RS has a BET surface area of 800 m^2/g, therefore our surface areas do not reach this maximum due to the mixture of cage types within our racemic crystals. With prolonged solvothermal treatment time, the surface areas steadily decrease to 401 m^2/g. This decrease can be explained by both the large increase in crystal size, and crystallinity, with respect to solvothermal synthesis time.[28] In addition, the isotherms in **Figure S12** no longer exhibit a type I isotherm, and instead, they begin to exhibit a type II isotherm with hysteresis. **Figure S13** contains the pore distributions of each sample. With an increase of solvothermal treatment, an increase in mesoporosity is introduced into this system, with broader pore distributions. Therefore, in terms of pore size distribution, the synthesized samples show "poor crystalline" CC3-R crystal structure.[15] This effect is also consistent with reports from Slater *et al.*,[5] and our discussion on the increase in concentration of the heterochiral cages.

To learn more about the correlation between DMF and the formation of different chiral cages, additional experiment were carried out. Specifically, two sets of experiments were done. In the first set of experiments, the composition of the solvent (different % of DMF from 100% to 0% (pure DCM)) were studied, keeping the solvothermal temperature, and synthesis time constant. In the second set of experiments, the solvothermal temperature was varied, while keeping solvent composition, and synthesis time constant. The second set of experiments was repeated, with a

different composition of solvent (100% DCM vs. 100% DMF). The synthesis conditions for each experiment are summarized in Table S2.

Figure S14 illustrates the correlation between the actual yield obtained for the precipitate, and filtered portion of the entire sample, as a function of solvent composition. Here, DMF was varied from 0-100% of the total solvent volume for samples A-D, and K. Solvothermal temperature and synthesis time were kept constant at 100°C, and 16 hours, respectively. At 0% DMF, (100% DCM) the actual yields for the precipitate, and filtrate were very similar. As the composition increases to 100% DMF, the trend shifts towards a higher amount of obtained filtered product, while the amount of precipitates collected after centrifugation was very small in comparison. This observation indicates that the amount of precipitates (CC3-R/CC3-S), which have a very low solubility in most solvents, was much lower than the amount of soluble cages collected from the filtrate of the supernatant species after precipitation with hexane. Figure S15 summarizes the yield of precipitate product, with respect to solvothermal temperature. Here, composition of DMF is either 100%, or 0%. This drastic difference in solvent environment, has an impact on the almost symmetrical opposition in the precipitate yields as a function of temperature. Specifically, at 120°C, the amount of precipitate collected from a 100% DCM solvent environment was about 75%, while the amount collected in 100% DMF was less than 10%. Actual yields of both the precipitate, and filtered product for 100% DCM experiments followed the same trend, while in 100% DMF, the product yields oppose one another. Although the actual total yield is low for the DMF experiments, more soluble product was recovered after precipitation with hexane, and filtration, rather than with centrifugation at higher temperatures.

Figures S16-S19 show XRD patterns, and representative SEM images of each sample (Table S2) separated into its respective components. In some cases, a component XRD pattern was omitted due to scarcity of product for proper XRD collection. SEM images of the precipitated products are also shown. XRD patterns of the precipitate suggest that the sample synthesized with DCM (sample A) corresponds to alpha phase, while the sample synthesized with DMF suggests the presence of alpha and dissymmetric cage structure. Rietveld refinement calculations indicate that for this sample, the percentages of alpha and dissymmetric phases are 68 % and 32% respectively. Interestingly samples with different contents of DMF (samples C,K,B) also show the presence of these two phases. The effect of solvothermal temperature when employing DCM as solvent (samples S,T,U) was minimum. In other words, independently of temperature these samples (precipitate) were highly crystalline displaying the alpha phase. In the case of samples synthesized in the presence of DMF, temperature had a profound effect. Specifically, poorly crystalline XRD patterns for the precipitate were obtained at lower temperatures (samples O,P). The higher temperature led to crystalline alpha, and dissymmetric phases for the precipitate. From SEM images, samples synthesized with traditional DCM (sample A) solvent lead to more regular morphologies and faceted crystals as compared to the sample synthesized with DMF (sample D). In general, the samples synthesized with different contents of DMF and DMC (Samples C, K, and B) show a mixture of morphologies consisted on octahedral, irregular and plate-like shapes. The lower the amount of DMF, the more regular crystals were observed. In the case of the effect of solvothermal temperature, when DCM was used as solvent (samples S,T,U) the size, and shape of the resultant CC3 crystals remained almost unaltered. However, in the case in which DMF (samples O,P,R) was used as solvent, higher solvothermal temperatures led to larger and more irregular crystals. Figure S20, and S21 show 1D 1H NMR spectra for the filtrate, and filtered product, consistent with the formation of CC3 cages.

In conclusion, we have demonstrated that a prototypical porous organic cage CC3, can be synthesized in the presence of a non-traditional solvent, (DMF). By changing the solute supersaturation in solution, we were able to modify crystallization kinetics, which affected the resultant textural, morphological and structural properties of the precipitated crystals. Upon solvothermal treatment, the relative crystallinity of CC3-R/CC3-S, increased with respect to synthesis time, which was confirmed by the steady decrease of BET surface areas, and sharpening of PXRD peaks. Prolonged solvothermal treatment in the presence of DMF led to higher concentrations of the soluble heterochiral cage product CC3-SR/CC3-RS, due to increased DMF-linker interactions, and higher reaction reversibility. In general, under similar experimental conditions, when DMF was used as solvent, a mixture of alpha and dissymmetric cage structure was observed. In the presence of traditional DCM solvent pure alpha phase is observed. Solvothermal temperature had a profound effect when DMF was used as solvent. Specifically, higher solvothermal temperatures led to enhanced crystallinity on the resultant alpha, and dissymmetric phases. In the case of DCM employed as solvent, independently of temperature the resultant precipitates were highly crystalline displaying the alpha phase. To the best of our knowledge, this is the first report of this type of approach for CC3 synthesis, and can be used as a tool to change the kinetics of the type of products synthesized in solution. Currently, we are exploring the synthesis of other representative POC systems in the presence of DMF.

There are no conflicts to declare. M.A.C. gratefully thanks the Department of Energy (DOE) Nuclear Energy University Program (NEUP) under Grant No. DE-NE0008429 for financial support.

Notes and references

1. T. Tozawa, J. T. A. Jones, S. I. Swamy, S. Jiang, D. J. Adams, S. Shakespeare, R. Clowes, D. Bradshaw, T. Hasell, S. Y. Chong, C. Tang, S. Thompson, J. Parker, A. Trewin, J. Bacsa, A. M. Z. Slawin, A. Steiner and A. I. Cooper, Nat. Mater., 2009, 8, 973-978.

2. M. A. Little, S. Y. Chong, M. Schmidtmann, T. Hasell and A. I. Cooper, Chem. Commun., 2014, 50, 9465-9468.

3. T. Hasell and A. I. Cooper, Nat. Rev. Mater., 2016, 1, 14.

4. M. Liu, M. A. Little, K. E. Jelfs, J. T. A. Jones, M. Schmidtmann, S. Y. Chong, T. Hasell and A. I. Cooper, J. Am. Chem. Soc. , 2014, 136, 7583-7586.

5. A. G. Slater, M. A. Little, M. E. Briggs, K. E. Jelfs and A. I. Cooper, Mol. Syst. Des. Eng., 2018, 3, 223-227.

6. T. Hasell, M. Miklitz, A. Stephenson, M. A. Little, S. Y. Chong, R. Clowes, L. J. Chen, D. Holden, G. A. Tribello, K. E. Jelfs and A. I. Cooper, J. Am. Chem. Soc., 2016, 138, 1653-1659.

7. T. Hasell, J. A. Armstrong, K. E. Jelfs, F. H. Tay, K. M. Thomas, S. G. Kazarian and A. I. Cooper, Chem. Commun., 2013, 49, 9410-9412.

8. J. K. Sun, W. W. Zhan, T. Akita and Q. Xu, J. Am. Chem. Soc., 2015, 137, 7063-7066.

9. Y. Zhang, Y. Xiong, J. Ge, R. Lin, C. Chen, Q. Peng, D. S. Wang and Y. D. Li, Chem. Commun., 2018, 54, 2796-2799.

10. A. G. Slater, P. S. Reiss, A. Pulido, M. A. Little, D. L. Holden, L. Chen, S. Y. Chong, B. M. Alston, R. Clowes, M. Haranczyk, M. E. Briggs, T. Hasell, G. M. Day and A. I. Cooper, ACS Cent. Sci., 2017, 3, 734-742.

11. G. H. Zhu, C. D. Hoffman, Y. Liu, S. Bhattacharyya, U. Tumuluri, M. L. Jue, Z. L. Wu, D. S. Sholl, S. Nair, C. W. Jones and R. P. Lively, Chem. Eur. J., 2016, 22, 10743-10747.

12. Y. Liu, G. Zhu, W. You, H. Tang, C. W. Jones, R. P. Lively and D. S. Sholl, J. Phys. Chem. C , 2018.

13. L. Chen, P. S. Reiss, S. Y. Chong, D. Holden, K. E. Jelfs, T. Hasell, M. A. Little, A. Kewley, M. E. Briggs, A. Stephenson, K. M. Thomas, J. A. Armstrong, J. Bell, J. Busto, R. Noel, J. Liu, D. M. Strachan, P. K. Thallapally and A. I. Cooper, Nat. Mater., 2014, 13, 954-960.

14. S. Komulainen, J. Roukala, V. V. Zhivonitko, M. A. Javed, L. J. Chen, D. Holden, T. Hasell, A. Cooper, P. Lantto and V. V. Telkki, Chem. Sci., 2017, 8, 5721-5727.

15. T. Hasell, S. Y. Chong, K. E. Jelfs, D. J. Adams and A. I. Cooper, J. Am. Chem. Soc , 2012, 134, 588-598.

16. J. T. A. Jones, T. Hasell, X. Wu, J. Bacsa, K. E. Jelfs, M. Schmidtmann, S. Y. Chong, D. J. Adams, A. Trewin, F. Schiffman, F. Cora, B. Slater, A. Steiner, G. M. Day and A. I. Cooper, Nature, 2011, 474, 367.

17. X. Feng, Z. Zong, S. K. Elsaidi, J. B. Jasinski, R. Krishna, P. K. Thallapally, M. A. Carreon, J. Am. Chem. Soc, 2016, 138, 9791-9794.

18. M. Shah, H. T. Kwon, V. Tran, S. Sachdeva and H.-K. Jeong, Microporous Mesoporous Mater, 2013, 165, 63-69.

19. G. C. Bleier, J. Watt, C. K. Simocko, J. M. Lavin and D. L. Huber, Angew. Chem. Int., 2018, 57, 7678-7681.

20. V.V. Guliants, and M. A. Carreon, Catalysis 2005, 18, 1-45.

21. S. Hu, M. Liu, X. Guo, K. Li, Y. Han, C. Song and G. Zhang, Cryst Growth Des., 2017, 17, 6586-6595.

22. S. R. Venna and M. A. Carreon, J. Phys. Chem. C , 2008, 112, 16261-16265.

23. X. Feng, T. Wu and M. A. Carreon, J. Cryst. Growth., 2016, 455, 152-156.

24. J. D. F. Ramsay and S. Kallus, in Membrane Science and Technology, ed. N. K. Kanellopoulos, Elsevier, 2000, vol. 6, pp. 373-395.

25. E. Berardo, L. Turcani, M. Miklitz and K. E. Jelfs, Chem. Sci., 2018, 9, 8513-8527.

26. E. Berardo, R. L. Greenaway, L. Turcani, B. M. Alston, M. J. Bennison, M. Miklitz, R. Clowes, M. E. Briggs, A. I. Cooper and K. E. Jelfs, Nanoscale, 2018, 10, 22381-22388.

27. V. Santolini, M. Miklitz, E. Berardo and K. E. Jelfs, Nanoscale, 2017, 9, 5280-5298.

28. J. Lucero, S. K. Elsaidi, R. Anderson, T. Wu, D. A. Gomez-Gualdron, P. K. Thallapally and M. A. Carreon, Cryst Growth Des., 2018, 18, 921-927.

29. G. H. Zhu, Y. Liu, L. Flores, Z. R. Lee, C. W. Jones, D. A. Dixon, D. S. Sholl and R. P. Lively, Chem. Mater., 2018, 30, 262-272.

30. S. Jiang, Q. L. Song, A. Massey, S. Y. Chong, L. J. Chen, S. J. Sun, T. Hasell, R. Raval, E. Sivaniah, A. K. Cheetham and A. I. Cooper, Angew. Chem. Int., 2017, 56, 9391-9395.

31. M. E. Briggs and A. I. Cooper, Chem. Mater., 2017, 29, 149-157.

TOC Figure

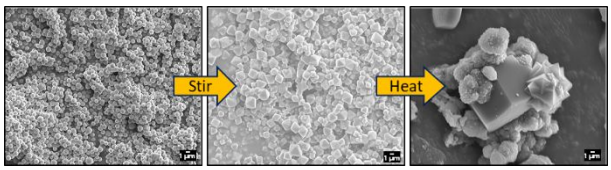

Morphology, and crystal product of Porous Organic Cage CC3, was modified by the use of a novel and non-traditional high dielectric constant solvent dimethyl formamide.